

Title: Point-surface fusion of station measurements and satellite observations for mapping PM_{2.5} distribution in China: methods and assessment

Authors: Tongwen Li ^a, Huanfeng Shen ^{a,b,c,*}, Chao Zeng ^d, Qiangqiang Yuan ^e, Liangpei Zhang ^{b,f}

Affiliations:

^a School of Resource and Environmental Sciences, Wuhan University, Wuhan, Hubei, 430079, China.

^b The Collaborative Innovation Center for Geospatial Technology, Wuhan, Hubei, 430079, China.

^c The Key Laboratory of Geographic Information System, Ministry of Education, Wuhan University, Wuhan, Hubei, 430079, China.

^d The State Key Laboratory of Hydrosience and Engineering, Department of Hydraulic Engineering, Tsinghua University, Beijing, 100084, China.

^e School of Geodesy and Geomatics, Wuhan University, Wuhan, Hubei, 430079, China.

^f The State Key Laboratory of Information Engineering in Surveying, Mapping and Remote Sensing, Wuhan University, Wuhan, Hubei, 430079, China.

Email address:

litw@whu.edu.cn (Tongwen Li), shenhf@whu.edu.cn (Huanfeng Shen),
zengchaozc@hotmail.com (Chao Zeng), yqiang86@gmail.com (Qiangqiang Yuan),
zlp62@whu.edu.cn (Liangpei Zhang)

*** Corresponding author:**

Huanfeng Shen (shenhf@whu.edu.cn). Phone: +86-027-68778375

ABSTRACT

Fine particulate matter (PM_{2.5}, particulate matters with aerodynamic diameter less than 2.5 μm) is associated with adverse human health effects, and China is currently suffering from serious PM_{2.5} pollution. To obtain spatially continuous ground-level PM_{2.5} concentrations, several models established by point-surface fusion of ground station and satellite observations have been developed. However, how well do these models perform at national scale in China? Is there space to improve the estimation accuracy of PM_{2.5} concentration? The contribution of this study is threefold. Firstly, taking advantage of the newly established national monitoring network, we develop a national-scale generalized regression neural network (GRNN) model to estimate PM_{2.5} concentrations. Secondly, different assessment experiments are undertaken in time and space, to comprehensively evaluate and compare the performance of the widely used models. Finally, to map the yearly and seasonal mean distribution of PM_{2.5} concentrations in China, a pixel-based merging strategy is proposed. The results indicate that the conventional models (linear regression, multiple linear regression, and semi-empirical model) do not perform well at national scale, with cross-validation R values of 0.488~0.552 and RMSEs of 30.80~31.51 $\mu\text{g}/\text{m}^3$, respectively. In contrast, the more advanced models (geographically weighted regression, back-propagation neural network, and GRNN) have great advantages in PM_{2.5} estimation, with R values ranging from 0.610 to 0.816 and RMSEs from 20.93 to 28.68 $\mu\text{g}/\text{m}^3$, respectively. In particular, the proposed GRNN model obtains the best performance. Furthermore, the mapped PM_{2.5} distribution retrieved from 3-km MODIS aerosol optical depth (AOD) products, agrees quite well with the station measurements. The results also show that our study has the capacity to provide reasonable information for the global monitoring of PM_{2.5} pollution in China.

Keywords: Satellite remote sensing; Point-surface fusion; AOD; PM_{2.5}; GRNN; Assessment

1. Introduction

Fine particulate matter (PM_{2.5}, particulate matters with aerodynamic diameter less than 2.5 μm) can carry toxic and harmful substances and travel across countries and geographic boundaries (Engel-Cox et al., 2013). Many epidemiological studies have shown that long-term exposure to PM_{2.5} is associated with adverse health effects (Bartell et al., 2013; Sacks et al., 2011). With the rapid economic development, China is suffering from serious air pollution, and PM_{2.5} has gradually become the primary pollutant, which has attracted widespread social concern (Peng et al., 2016; Yuan et al., 2012). Consequently, PM_{2.5} has been incorporated into the new air quality standard of the Chinese government (GB 3095-2012). Since January 2013, hourly PM_{2.5} concentrations have been disclosed to the public through the Chinese National Environmental Monitoring Center website (<http://www.cnemc.cn>). By the end of 2014, about 1500 monitoring sites had been established to report the overall air quality in China.

Despite the high precision and stability, there are still some limitations to spatiotemporal analysis due to the sparse and uneven distribution of the ground stations. Unlike the ground-level measurements, satellite-based observation has the capacity to provide wide-coverage data. Using both the ground station measurements and co-located satellite observations, the relationship between the various observed variables can be established. Based on this relationship and its variation rule in space, the spatially continuous data can be reconstructed. This method, which can generate data from point scale to surface scale, is known as “point-surface fusion”. The point-surface fusion of station-level PM_{2.5} measurements and satellite-based aerosol optical depth (AOD, also called aerosol optical

thickness) can obtain spatially continuous $PM_{2.5}$ data, and has the potential to compensate for the spatiotemporal limitation. Several widely used models, established by point-surface fusion, have been developed to describe the relationship between PM and AOD (AOD-PM relationship) (Beloconi et al., 2016; Chu et al., 2003; Gupta et al., 2006; Hoff and Christopher, 2009; Kloog et al., 2014; Li et al., 2011; Li et al., 2005; Liu et al., 2007; Martin, 2008).

According to a previous study (Lin et al., 2015), the existing models, which were developed to retrieve ground-level $PM_{2.5}$ concentrations using satellite observations, can be classified into two main categories: simulation-based models and observation-based models. Simulation-based models (Geng et al., 2015; Liu et al., 2004; van Donkelaar et al., 2010) consider the effects of both meteorology and aerosol properties, which are simulated with global or regional chemical transport models. They would be most suitable for predicting $PM_{2.5}$ concentration if we have comprehensive datasets (especially emission inventories) and a good understanding of the $PM_{2.5}$ formation and removal processes. Given the complexity of the problem, an observation-based model is a good compromise (Gupta and Christopher, 2009a). Observation-based models rely on the statistical relationship between AOD and in-situ $PM_{2.5}$ measurements, and are much easier to implement, but with an almost equivalent accuracy of $PM_{2.5}$ estimation. Hence, the observation-based models, established by point-surface fusion, have been extensively discussed and studied. Using a simple linear regression model between AOD and $PM_{2.5}$, early studies obtained some reasonable results (Chu et al., 2003; Guo et al., 2009; Li et al., 2005; Wang and Christopher, 2003; Wang et al., 2010). However, the relationship tends to be influenced by region and time due to the effects of variations in emissions and meteorological conditions. Through incorporating more

meteorological parameters (e.g., relative humidity, temperature, wind speed), a multiple linear regression model may better represent the AOD-PM_{2.5} relationship (Benas et al., 2013; Gupta and Christopher, 2009b). Unlike the empirical models, semi-empirical models take the related physical understanding into account (Emili et al., 2010; Liu et al., 2005; Tian and Chen, 2010; You et al., 2015b), and attempt to introduce physical prior knowledge to solve the problem. More recently, allowing for the spatial heterogeneity of the AOD-PM_{2.5} relationship, a more advanced statistical model called geographically weighted regression (GWR) has been developed to estimate PM_{2.5} concentration (Hu et al., 2013; Ma et al., 2014; Song et al., 2014; You et al., 2015b). This model predicts PM_{2.5} concentration using a local regression approach instead of globally constant regression parameters. In addition, as one of the intelligent algorithms, artificial neural networks (ANNs) have the potential to better represent the complex nonlinear relationship. Hence, ANNs have been introduced into the estimation of PM_{2.5} concentration (Gupta and Christopher, 2009a; Wu et al., 2012; Yao and Lu, 2014), which has been gradually considered to be a multi-variable and nonlinear problem. Furthermore, some more complex mixed effects models and generalized additive mixed models (GAM) have been developed (Kloog et al., 2011; Liu et al., 2009; Ma et al., 2016). On the other hand, considering the effect of the main aerosol characteristics, an observation-based method was developed by establishing a multi-parameter remote sensing formula of PM_{2.5} concentration (Li et al., 2016; Lin et al., 2015; Zhang and Li, 2015). All these observation-based models have been widely used, and have played an irreplaceable role in satellite-based estimation of PM_{2.5} concentration.

China is now facing a serious PM_{2.5} pollution problem (Peng et al., 2016; Zhang and Cao,

2015). Due to the wide geographical range and complex terrain, mapping the distribution of $PM_{2.5}$ concentration in China is faced with lots of challenges. To date, many researchers have made attempts to study the AOD-PM relationship in China (Guo et al., 2009; Li et al., 2011; Li et al., 2005; Lin et al., 2015; Ma et al., 2014; Ma et al., 2016; Song et al., 2014; Wang et al., 2010; Wu et al., 2012). Due to the unavailability of sufficient $PM_{2.5}$ measurements in China before 2013, most studies used a limited number of ground-level $PM_{2.5}$ measurements at a regional scale. However, the regional estimation and analysis of $PM_{2.5}$ concentration cannot provide sufficient information for the macroscopical monitoring of the whole of China. With the newly available national $PM_{2.5}$ measurements since January 2013, a few attempts have been made to estimate $PM_{2.5}$ concentration at national scale. However, their methods and data used to establish the AOD- $PM_{2.5}$ relationship differ greatly from one another. Additionally, the validation schemes of models have many differences; for instance, some schemes undertook validation based on yearly/monthly average, and some on a daily basis. Thus, the intercomparison of national-scale model performance is not possible. Furthermore, previous studies (Hoff and Christopher, 2009) have suggested that the models may perform differently in different regions. As a result, the performance of models developed in regional studies needs to be evaluated and compared at national scale. On the other side, although the widely used models have achieved reasonable results under certain conditions, the estimation accuracy of $PM_{2.5}$ concentration still has room for improvement (De Leeuw et al., 2006; Song et al., 2014).

In this paper, one of the main objectives is to introduce an advanced model (generalized regression neural network, GRNN), which can better represent the AOD- $PM_{2.5}$ relationship,

into the prediction of $PM_{2.5}$ distribution in China. Another main objective is to comprehensively evaluate and analyze the performance of the widely used mainstream models at national scale. Finally, a direct average only reflects the level of $PM_{2.5}$ pollution on those days with valid AOD data, so a pixel-based merging strategy is proposed to map the yearly and seasonal mean distribution of $PM_{2.5}$ concentrations.

2. Data and measurements

To estimate $PM_{2.5}$ concentration in China, the retrieval models were established using multi-source data. Some information of the various data sources is shown in Table 1, and further details are provided in Sections 2.1 to 2.3.

Table 1. Some information of various data used in statistic models to estimate $PM_{2.5}$ in China

Data	Frequency	Source
$PM_{2.5}$	Daily average	About 1500 air quality monitoring sites (in 2014) in China mainland
AOD	Daily	MODIS Terra and Aqua satellite
Meteorological data	Daily	MERRA-2 reanalysis data

2.1. Ground-level $PM_{2.5}$ measurements

Daily average $PM_{2.5}$ concentration data from February 2013 to December 2014 were obtained from the Chinese National Environmental Monitoring Center (CNEMC) website (<http://www.cnemc.cn>). With a spatial coverage of the whole of China (excluding Hong Kong, Macao, and Taiwan), the monitoring network is being continuously updated, and the number of monitoring sites has increased from ~500 in early 2013 to ~1500 by the end of 2014. According to the Chinese National Ambient Air Quality Standard (CNAAQs, GB3905-2012), the ground-level $PM_{2.5}$ concentration should be measured by the tapered element oscillating microbalance method (TEOM) or with beta attenuation monitors (BAM or beta-gauge), with

an uncertainty of 0.75% for the hourly record (Engel-Cox et al., 2013; Lin et al., 2015). Fig. 1 shows the spatial distribution of PM_{2.5} monitoring sites in China.

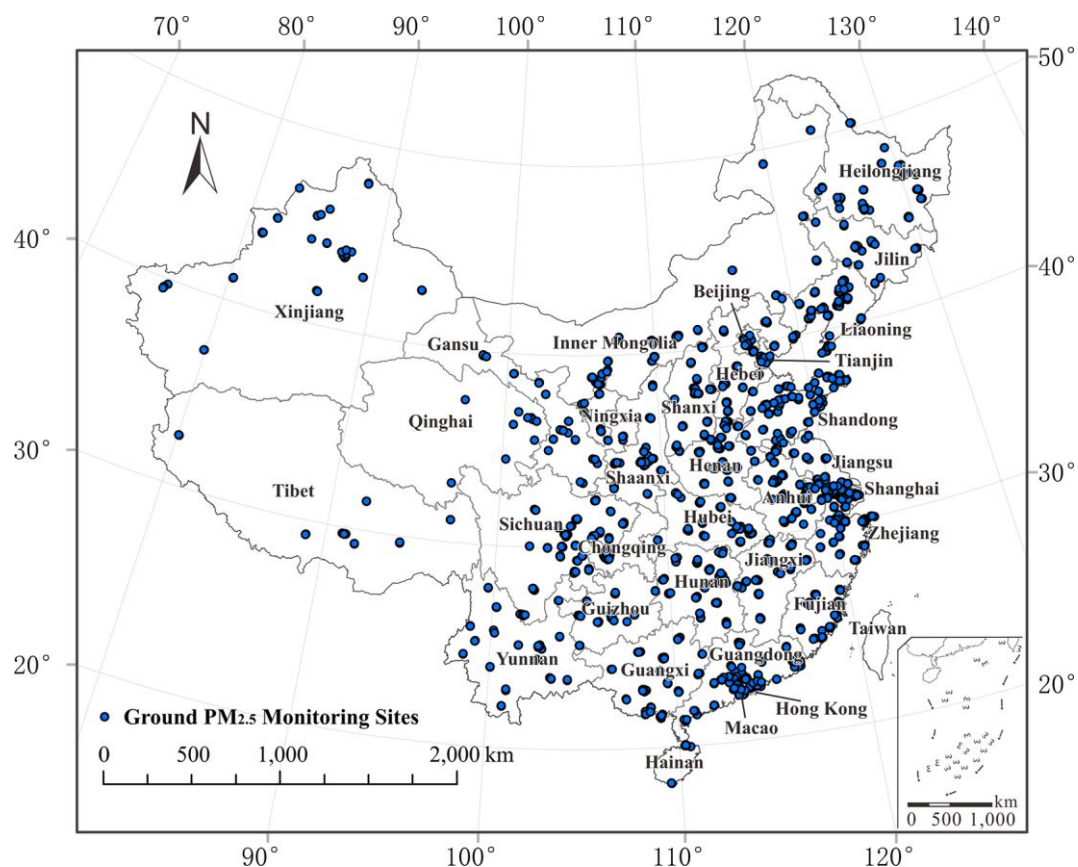


Fig. 1. Spatial distribution of PM_{2.5} monitoring sites in China, as of the end of 2014.

2.2. MODIS AOD products

The Moderate Resolution Imaging Spectroradiometer (MODIS) aboard the National Aeronautics and Space Administration (NASA)'s Earth Observing System (EOS) satellites, Terra and Aqua, can provide retrieval products of aerosol and cloud properties with nearly daily global coverage (Remer et al., 2005). Recently, a new version of MODIS aerosol products (Collection 6) is released at a higher spatial resolution (3 km at nadir). Both the newly released 3-km and the prior standard 10-km AOD products are retrieved using the dark target algorithm, whereas a single retrieval box of 6×6 pixels and 20×20 pixels is averaged, respectively. Moreover, the pixels outside the reflectivity range of the brightest 50% and

darkest 20% at $0.66 \mu m$ are discarded to reduce uncertainty for the 3-km AOD products (Levy et al., 2013; Livingston et al., 2014).

In our study, both MODIS Terra and Aqua 3-km AOD products, corresponding to the ground $PM_{2.5}$ measurements in space and time, are downloaded from Level 1 and Atmosphere Archive and Distribution System (LAADS) website (<http://ladsweb.nascom.nasa.gov>). The coverage of these two AOD products differs because of the different crossing times of the two sensors. Hence, linear regression analysis are conducted between those pixels where both AOD products are present for each day, and the regression coefficients are used to predict the missing Aqua AOD values from corresponding available Terra AOD, and vice versa (Hu et al., 2014b; Ma et al., 2014). Then the average of two AOD products are employed to estimate daily average $PM_{2.5}$ concentration.

2.3. Meteorological data

In our study, the NASA atmospheric reanalysis data called the second Modern-Era Retrospective analysis for Research and Applications (MERRA-2) (Molod et al., 2015; Rienecker et al., 2011) is used. It uses the Goddard Earth Observing System Model, Version 5 (GEOS-5) data assimilation system, which is able to use the newer microwave sounders and hyperspectral infrared radiance instruments, as well as other data types. The MERRA-2 meteorological data are available from 1980, with a spatial resolution of 0.625° longitude \times 0.5° latitude. More details about the MERRA-2 data can be found at the website (http://gmao.gsfc.nasa.gov/GMAO_products/).

We extracted relative humidity (RH, %), air temperature at 2m height (TEMP, K), wind speed at 10 m above ground (WS, m/s), surface pressure (SP, Pa), and planetary boundary

layer height (HPBL, m) between 10 am and 11 am local time (Terra satellite overpass time corresponds to 10:30 am local time), and 1 pm and 2 pm local time (Aqua satellite overpass time corresponds to 1:30 pm local time), respectively. Each meteorological parameter were averaged over the two period to supplement the predictors for the daily average estimation of $PM_{2.5}$ concentration.

2.4. Data preprocessing and matching

All data above are re-processed to be consistent temporally and spatially to form a complete dataset which serves as the foundational samples for model development. Firstly, the satellite AOD and meteorological reanalysis data are regridded to 0.3 degree. Secondly, all data are re-projected to the same projection coordinate system. Finally, ground $PM_{2.5}$ measurements are associated with the value of satellite AOD and meteorological data covering the station. The averaging over multiple pixels is expected to effectively reduce random errors, but the best size of a single window centered at a given $PM_{2.5}$ monitoring site still remains unclear for our analysis. Hence, three different window sizes of 1×1 , 3×3 , 5×5 pixels were applied here, respectively, and with consistence to previous studies (Wu et al., 2012; You et al., 2015b), the average scheme over a window size of 3×3 pixels reported a slight advantage. After data preprocessing and matching, a total of 77978 records from multi-source data, which spans almost 2 years and contains ground-level $PM_{2.5}$, satellite-based AOD, MERRA meteorological reanalysis data, were collected for model development.

3. Methodology

3.1. Previous retrieval models

Many different models have been developed to estimate $PM_{2.5}$ concentration at both

regional and national scales, ranging from single-variable to multi-variable models, and including both linear and nonlinear models. In this study, the following widely used models were evaluated and compared.

3.1.1. Corrected linear regression (CLR)

The linear regression model was used in earlier studies to describe the AOD-PM relationship (Chu et al., 2003; Wang and Christopher, 2003). Later studies reported better performances after meteorological correction (Li et al., 2005; Wang et al., 2010). Hence, corrected linear regression model was used:

$$PM'_{2.5} = a + b \cdot \frac{AOD}{HPBL} \quad (1)$$

$$PM'_{2.5} = PM_{2.5} \cdot \left(\frac{1}{1 - RH/100} \right) \quad (2)$$

where AOD is the aerosol optical depth, and $PM'_{2.5}$ denotes the RH-corrected $PM_{2.5}$.

3.1.2. Multiple linear regression (MLR)

Through incorporating more meteorological parameters, MLR has been introduced into the prediction of $PM_{2.5}$ concentration (Benas et al., 2013; Gupta and Christopher, 2009b). Based on empirical statistics, it can be defined as:

$$PM_{2.5} = \beta_0 + \beta_1 \cdot AOD + \beta_2 \cdot TEMP + \beta_3 \cdot RH + \beta_4 \cdot WS + \beta_5 \cdot HPBL + \beta_6 \cdot SP \quad (3)$$

where β_0 is the interception for $PM_{2.5}$ prediction, and $\beta_1 \sim \beta_6$ are regression coefficients for the predictor variables.

3.1.3. Semi-empirical model (SEM)

Based on related physical understanding and statistical theory, SEM was developed to describe the relationship between meteorological observations, AOD, and $PM_{2.5}$ (Emili et al., 2010; Liu et al., 2005; Tian and Chen, 2010; You et al., 2015a). It can be expressed as:

$$PM_{2.5} = e^{\beta_0 + \beta_2 \cdot TEMP + \beta_3 \cdot RH} \cdot AOD^{\beta_1} \cdot WS^{\beta_4} \cdot HPBL^{\beta_5} \quad (4)$$

3.1.4. Geographically weighted regression (GWR)

The GWR model was developed to account for the spatial heterogeneity of the AOD-PM_{2.5} relationship (Hu et al., 2013; Ma et al., 2014; Song et al., 2014; You et al., 2015b). Unlike the previous models, GWR does not predict PM_{2.5} concentration using globally constant parameters, but generates continuous parameters by local model fitting. It can be represented as Eq. (5):

$$PM_{2.5,i} = \beta_{0,i} + \beta_{1,i} \cdot AOD + \beta_{2,i} \cdot TEMP + \beta_{3,i} \cdot RH + \beta_{4,i} \cdot WS + \beta_{5,i} \cdot HPBL + \beta_{6,i} \cdot SP \quad (5)$$

where the meanings of the variables and coefficients are the same as Eq. (3), but based on local regression over monitoring station i , hence the coefficients vary in space. In our study, the adaptive bandwidths were used because of the uneven distribution of the PM_{2.5} stations.

3.1.5. Back-propagation neural network (BPNN)

An ANN can be considered as a set of computer algorithms designed to simulate biological neural networks in terms of machine learning and pattern recognition. Hence, ANNs have the potential to extract trends in imprecise and complicated nonlinear data (Gupta and Christopher, 2009a). With more and more predictors, the estimation of PM_{2.5} concentration has been gradually considered to be a multi-variable and nonlinear problem. Consequently, ANNs have been introduced into PM_{2.5} estimation (Gupta and Christopher, 2009a; Wu et al., 2012; Yao and Lu, 2014). The most common training algorithm is back-propagation (BP), a BPNN model with three layers (input layer, hidden layer, and output layer) was constructed in our study. The input parameters were latitude, longitude, month, AOD, TEMP, RH, WS, HPBL, and SP. According to previous studies (Gardner and Dorling, 1998; Reich et al., 1999), the number of nodes in the hidden layer ranges from $2\sqrt{n} + \mu$ to $2n + 1$, where n and μ

are the number of nodes in the input layer and output layer, respectively. Thus, the number of nodes in the hidden layer was varied from 7 to 19, and 18 nodes (which performed the best) were selected in this paper.

3.2. Proposed generalized regression neural network (GRNN) model

With extensive and comprehensive data, an ANN has the potential to describe the spatial and temporal variation of AOD-PM_{2.5} relationship. Previous studies (Gupta and Christopher, 2009a; Ordieres et al., 2005) have indicated that ANNs can outperform the classic statistical models. However, the well-known BPNN has the disadvantages of slow convergence velocity and easily converging to local minimum (Wen et al., 2000; Yu, 1992). Hence, we introduce here another neural network named the generalized regression neural network (GRNN), which can overcome the shortcomings of BPNN (Cigizoglu and Alp, 2006; Kisi and Kerem Cigizoglu, 2007). GRNN is often used for function approximation, and it can be considered as a normalized radial basis function (RBF) network. Based on a standard statistical technique called kernel regression, GRNN can solve any function approximation problem if sufficient data are given. A common GRNN architecture has three layers of neurons: the input layer, the RBF hidden layer, and the special linear output layer. The input layer and RBF hidden layer are usually connected by a density function such as the Gaussian density function. The output of the hidden layer is not directly connected to the output layer by a linear function, but is firstly connected by a transition of a dot function, reflecting the specialty of the output layer. Further theoretical details about GRNN can be found in previous studies (Specht, 1991; Specht, 1993).

In our study, the input signals are latitude, longitude, month, AOD, TEMP, RH, WS, HPBL,

and SP, and the output parameter is $PM_{2.5}$ concentration. The main function of the GRNN model is to estimate a nonlinear regression surface of $PM_{2.5}$ from these input signals. The input data are sent to the neural network, the output $PM_{2.5}$ concentrations can be calculated. They are compared with the in situ $PM_{2.5}$ data, and an error is estimated. The error is sent back to the GRNN model to adjust the weights to generate a more appropriate surface of $PM_{2.5}$ concentration. This process is therefore to find optimal value of weights to establish the nonlinear relationship between $PM_{2.5}$ and independent predictors. The GRNN model here predicts $PM_{2.5}$ concentration using AOD and meteorological parameters, which are primarily and supplementary predictors, respectively. In particular, allowing for the temporal and spatial variation of AOD- $PM_{2.5}$ relationship, the latitude, longitude, and month are also input to better estimate $PM_{2.5}$ concentration. Unlike BPNN, the number of nodes in the hidden layer of GRNN was obtained from training without artificial intervention; hence, GRNN was trained with few parameters set in advance. The schematics of GRNN used to estimate $PM_{2.5}$ concentration are presented in Fig. 2.

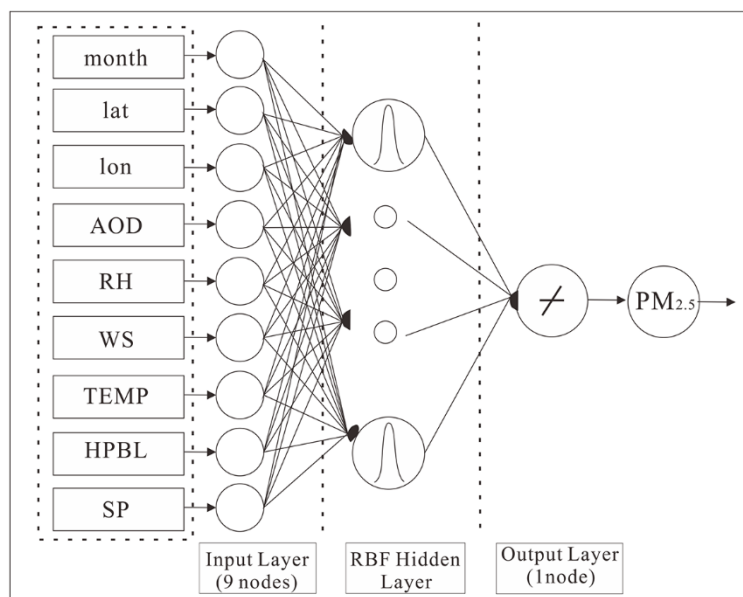


Fig. 2. Schematic of GRNN used to estimate $PM_{2.5}$ concentration in China.

3.3. Model validation

To validate the performance of the above models, the correlation coefficient (R) and root-mean-square error (RMSE) between the observed $PM_{2.5}$ and estimated $PM_{2.5}$ were adopted. Furthermore, a 10-fold cross-validation method (Rodriguez et al., 2010) was applied to test the model overfitting and predictive power. The dataset was averagely divided into 10 folds randomly. Nine folds of the dataset were used for model fitting, and one fold was predicted in each round of the cross-validation. This step was repeated 10 times until every fold was tested. Finally, R and RMSE values were calculated for the model fitting and cross-validation results, respectively, to evaluate the model performance.

3.4. Mapping strategy for the mean $PM_{2.5}$ distribution

The 3-km MODIS AOD products, retrieved by the dark target algorithm, share a generic feature with other standard AOD products, which is the absence of data due to clouds or high surface reflectance. Due to the absence of AOD data, the temporally continuous $PM_{2.5}$ data cannot be retrieved at the same location. When we map the temporal mean distribution of $PM_{2.5}$ concentration, a direct average can only reflect the level of $PM_{2.5}$ pollution on certain days. To address this issue, a pixel-based merging strategy is proposed, referring to the related studies of spatiotemporal fusion (Shen et al., 2013; Wu et al., 2013; Wu et al., 2015). Firstly, a spatial $PM_{2.5}$ map on every day can be interpolated by ground-station-level measurements. Due to the sparse distribution of the stations, this map is relatively coarse in space, but still keeps the temporal trend. Thus, the variation of the interpolated $PM_{2.5}$ remains equal to that of the satellite-derived $PM_{2.5}$ at the same location during the same period, and can be represented as Eq. (6),

$$L_{i,p} - L_{i,m} = F_{i,p} - F_{i,m} + \varepsilon_{i,m,p} \quad (6)$$

where $L_{i,m}$ denotes the PM_{2.5} at pixel i on day m interpolated by ground-station-level measurements using the inverse distance weighting (IDW) approach, and $F_{i,m}$ is the satellite-based estimation of PM_{2.5} at pixel i on day m , as are $L_{i,p}$ and $F_{i,p}$. $\varepsilon_{i,m,p}$ is the random error, which will be reduced or eliminated by temporally averaging. For pixel i , assuming that $F_{i,p}$ is missing and needs to be estimated, then m is the closest day with valid PM_{2.5} data at the same location to day p . Thus, the missing satellite-derived PM_{2.5} data can be reconstructed, and we can map the mean distribution of PM_{2.5} concentration in China.

Additionally, some previous studies (van Donkelaar et al., 2012; Zheng et al., 2016) used annual/seasonal mean surface PM_{2.5} measurements to correct this potential sampling biases. They calculate correction factors for each monitoring station/grid, then the factors are extrapolated to the entire study region. By applying the correction factors for each pixel/grid to predict annual/seasonal average PM_{2.5}, the bias-corrected PM_{2.5} concentration can be obtained. Hence, our mapping strategy is compared with this bias-correction method (we denote it as “BCM”).

4. Results and discussion

4.1. Assessment of the various models

4.1.1. Performance of the models

Table 2 shows the performance of various models. In model fitting, R values range from 0.485 to 0.895, and RMSEs from 16.51 to 31.64 $\mu\text{g} / \text{m}^3$. In the cross-validation results, a similar trend appears. Using simple linear regression, the CLR model performs the worst, with R and RMSE values of 0.488 and 31.51 $\mu\text{g} / \text{m}^3$ for cross-validation, respectively.

There is a large improvement (0.488 to 0.531 for R) from the CLR model to the MLR model, which considers more meteorological factors. Through introducing some physical prior knowledge, the SEM model has an advantage in PM_{2.5} estimation, with an R value of 0.552 and an RMSE of 30.80 $\mu\text{g} / \text{m}^3$, respectively. Unlike the above models, the GWR model incorporates spatial information into the AOD-PM_{2.5} relationship, and shows a large improvement over the SEM model, with R increasing by 0.058 and RMSE decreasing by 2.12 $\mu\text{g} / \text{m}^3$, respectively. As one of the intelligent algorithms, the BPNN model has the capacity to better represent the AOD-PM_{2.5} relationship, with R and RMSE values of 0.693 and 25.96 $\mu\text{g} / \text{m}^3$, respectively. Compared with the results of BPNN, R increases by 0.123 (from 0.693 to 0.816), and RMSE decreases by 5.03 $\mu\text{g} / \text{m}^3$ (from 25.96 to 20.93 $\mu\text{g} / \text{m}^3$) for cross-validation of the GRNN model. These findings suggest that the proposed GRNN model performs the best, followed by BPNN and GWR, and then SEM and MLR, whereas the simple CLR model obtains the worst performance at national scale.

Table 2. Performance of the various models.

	Model fitting (N=70180)		Cross-validation (N=77978)	
	R	RMSE ($\mu\text{g} / \text{m}^3$)	R	RMSE ($\mu\text{g} / \text{m}^3$)
CLR	0.485	31.64	0.488	31.51
MLR	0.530	30.52	0.531	30.52
SEM	0.551	30.78	0.552	30.80
GWR	0.624	28.23	0.610	28.68
BPNN	0.699	25.90	0.693	25.96
GRNN	0.895	16.51	0.816	20.93

Furthermore, it should be noted that the conventional models (CLR, MLR, and SEM) have all obtained reasonable results at regional scale in China (Li et al., 2005; Song et al., 2014; Wang et al., 2010), but do not perform well at national scale, with R values of 0.488~0.552 and RMSEs of 30.80~31.51 $\mu\text{g} / \text{m}^3$ for cross-validation. The results indicate that the

conventional models cannot adequately represent the association between $PM_{2.5}$ and independent variables at national scale. However, with R values ranging from 0.610 to 0.816 and RMSEs from 20.93 to $28.68 \mu g / m^3$, the more advanced models (GWR, BPNN, and GRNN) have a great advantage in the estimation of $PM_{2.5}$ concentration.

Allowing for the superiority of the GRNN model, we further evaluated and analyzed its performance. Fig. 3 shows the scatter plots for GRNN model fitting and cross-validation. The R and RMSE values for model fitting are 0.895 and $16.51 \mu g / m^3$, respectively. From model fitting to cross-validation, R decreases by 0.079 and RMSE increases by $4.42 \mu g / m^3$. The results demonstrate that the proposed model results in a slight overfitting (Hu et al., 2014a; Ma et al., 2014). However, with the highest R and lowest RMSE values for both model fitting and cross-validation, the proposed GRNN model outperforms the other models. Hence, despite a slight overfitting, the GRNN model is more effective for the estimation of $PM_{2.5}$ concentration in China.

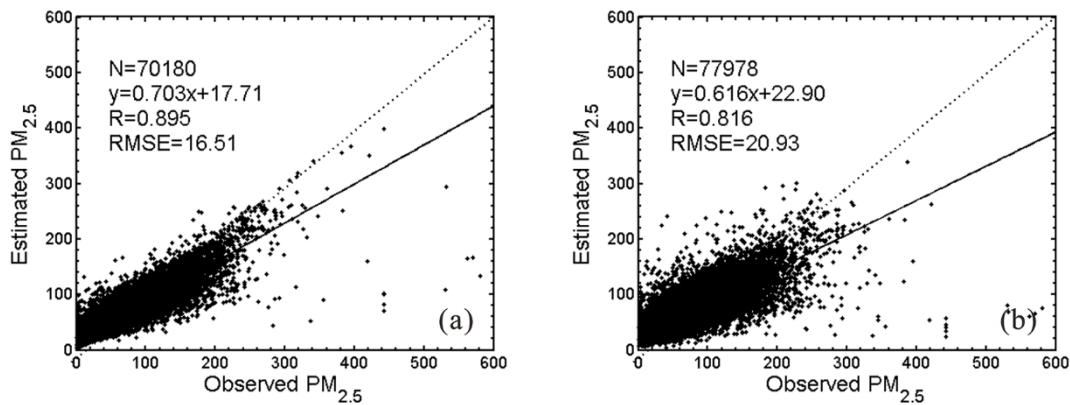


Fig. 3. Results of GRNN (a) model fitting and (b) cross-validation. $PM_{2.5}$ unit: $\mu g / m^3$. The dashed line is the 1:1 line as the preference.

To further analyze the spatial performance of the GRNN model, the R and RMSE values between the observed and estimated $PM_{2.5}$ over the stations were calculated and are presented

in Fig. 4. The correlation coefficients at 727 out of 828 stations are greater than 0.8, and 84.90% of the total stations report a low RMSE of less than $20 \mu\text{g} / \text{m}^3$. Spatially, the higher R values are clustered in Eastern China, suggesting the accurate estimation of $\text{PM}_{2.5}$ concentration in this area. In contrast, the lower R values are found in Northwest China, which is probably caused by the sparse distribution of the ground stations in this area. Moreover, a higher RMSE cluster appears in the Beijing-Tianjin-Hebei (BTH) region and its surroundings. However, it should be noted that the level of $\text{PM}_{2.5}$ concentration in the BTH region is relatively high (Lin et al., 2015; Ma et al., 2014).

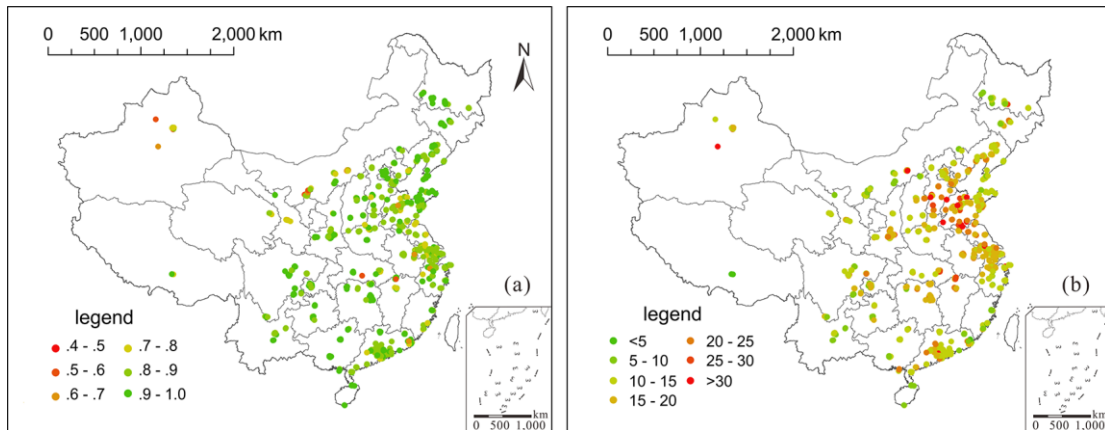


Fig. 4. Spatial distribution of (a) R and (b) RMSE ($\mu\text{g} / \text{m}^3$) between observed and estimated $\text{PM}_{2.5}$ over the stations.

4.1.2. Seasonal variation of model performance

Previous studies have shown that the models can perform differently as a function of the seasons (Gupta and Christopher, 2009a; Lin et al., 2015). Therefore, all the models were respectively established in each season to discuss and compare the seasonal variation of model performance. In our study, the seasons were defined as spring (March–May), summer (June–August), autumn (September–November), and winter (December–February), for which the numbers of data records were 21573, 23244, 26281, and 6880, respectively. Fig. 5 shows

the seasonal variation of model performance for cross-validation.

As shown in Fig. 5, the GRNN model performs the best in every season ($R= 0.822, 0.817, 0.828, \text{ and } 0.837$ for cross-validation in spring, summer, autumn, and winter, respectively), followed by BPNN and GWR, and then MLR and SEM, and the simple CLR model obtains the poorest performance (the R values of the four seasons are $0.351, 0.587, 0.569, \text{ and } 0.502$, respectively). The results demonstrate that by taking more meteorological parameters into consideration, the relatively advanced models can significantly improve the accuracy of $\text{PM}_{2.5}$ estimation. Furthermore, for each season, the GWR model performs a little worse than BPNN, but better than the conventional models, indicating that incorporating spatial information into the statistical model can better describe the AOD- $\text{PM}_{2.5}$ relationship. Among four seasons, all models have achieved the poorest performance in spring, probably caused by the influence of the enhanced contribution of dust particle (Zhang and Cao, 2015).

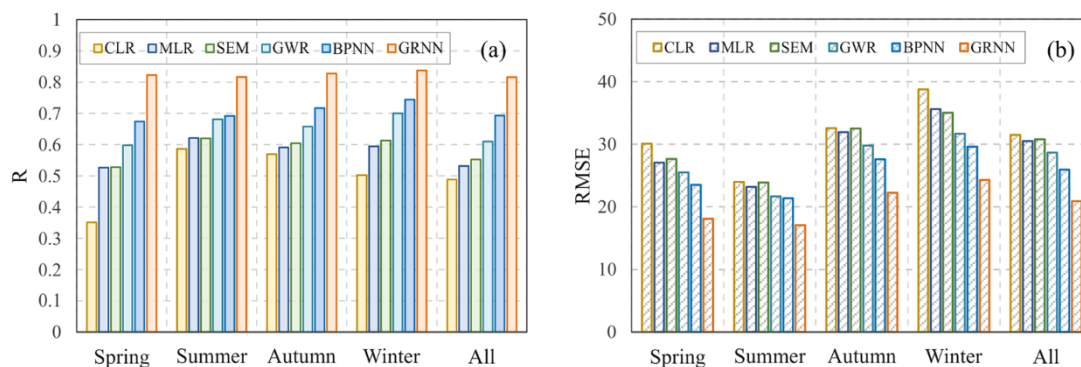


Fig. 5. Seasonal variation of (a) R and (b) $\text{RMSE} (\mu\text{g} / \text{m}^3)$ between observed and estimated $\text{PM}_{2.5}$.

On the other hand, all the models generally perform better at seasonal scale (except for spring) than yearly scale, reflecting the influence of the seasons on the AOD- $\text{PM}_{2.5}$ relationship. It should be noted that the conventional models (CLR, MLR, and SEM) reports a more significant improvement of R value from yearly scale to seasonal scale, indicating that they seem to be more suitable for seasonal observation than yearly observation.

4.1.3. Geographical variation of model performance

Geographical location is considered to be one of the factors which has an influence on the AOD-PM_{2.5} relationship (Hoff and Christopher, 2009; Ma et al., 2014). Clearly, China has a wide geographical range, and hence the models may perform differently in different regions. To explore the geographical variation of model performance, all the models were respectively established in every 4°×4° grid box, as in the study of Gupta and Christopher (2009b). All the data measured at the stations falling in each grid box were collected. However, some grid boxes containing only a few (<4) stations were eliminated. Fig. 6 shows the geographical variation of R values between observed and estimated PM_{2.5} for cross-validation, and the summary of the R and RMSE statistics over all the grid boxes is presented in Table 3.

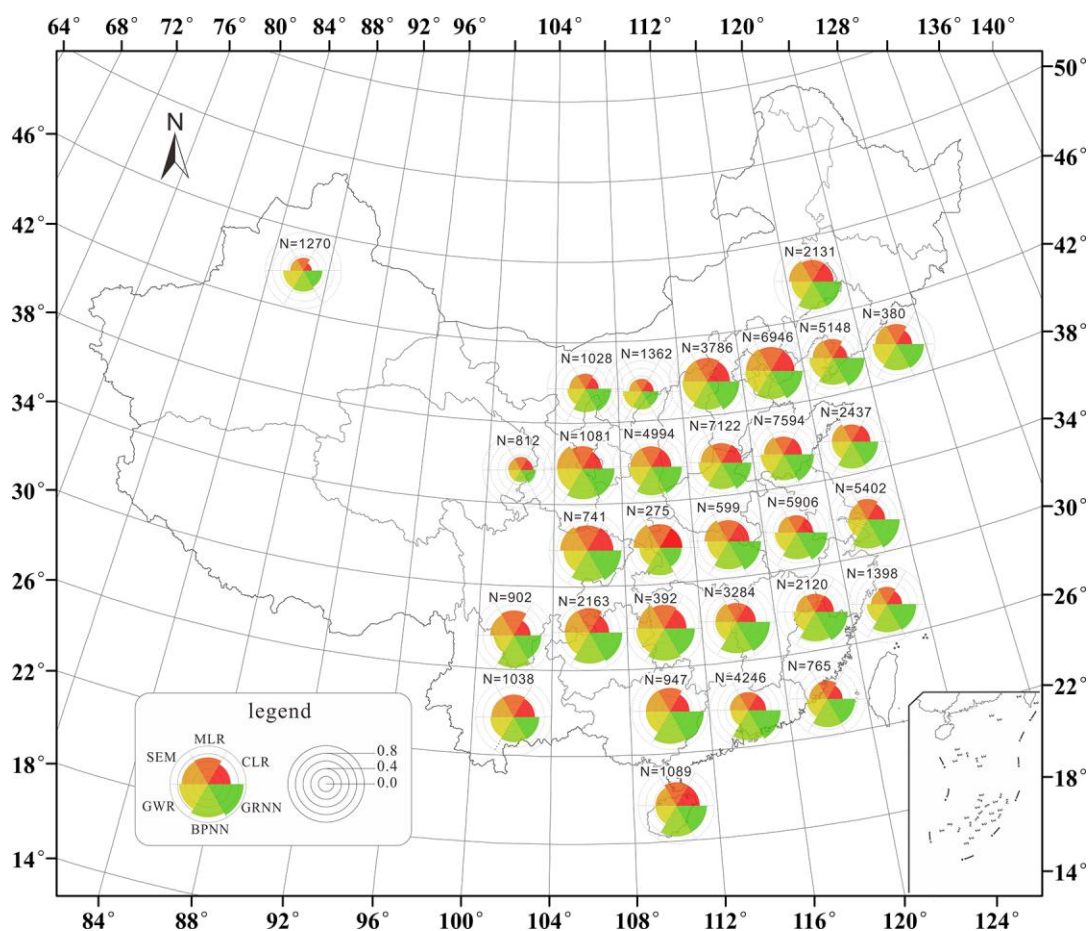


Fig. 6. Geographical variation of R values between observed and estimated PM_{2.5} in each 4°×4° grid box.

Compared with the performance of the various models at national scale, a similar trend can be investigated in most of the grid boxes. That is, the GRNN model performs the best, followed by BPNN and GWR, and CLR gives the poorest performance. However, the GWR model does not report great advantages over the conventional models, and the CLR model obtains almost the same performance as MLR. Additionally, some spatial differences are found. The GRNN model tends to obtain poorer results over the grid boxes in West China. This may be caused by the relatively sparse distribution of the PM_{2.5} monitoring stations in this area. The models, especially the neural network models (BPNN and GRNN), achieve the highest accuracies and stability of performance over those grid boxes which locate between longitudes 112 ° and 120 °, which contain more data records. These findings indicate that with more comprehensive data, the neural network models can perform better accordingly.

Table 3. Summary of the R and RMSE statistics over all the grid boxes.

	R						RMSE ($\mu\text{g} / \text{m}^3$)					
	CLR	MLR	SEM	GWR	BPNN	GRNN	CLR	MLR	SEM	GWR	BPNN	GRNN
Minimum	0.219	0.328	0.336	0.320	0.317	0.386	14.87	14.58	14.75	13.49	11.64	12.30
Maximum	0.681	0.657	0.710	0.739	0.848	0.887	37.55	36.73	37.51	35.77	31.31	35.34
Mean	0.482	0.523	0.546	0.568	0.719	0.754	27.41	26.54	26.53	25.46	21.37	20.26
Sd	0.103	0.095	0.105	0.079	0.113	0.130	5.34	5.61	5.43	5.49	4.72	4.76

As Table 3 shows, the R value of the GRNN model ranges from 0.386 to 0.887, with a mean value of 0.754. There is a large decrease (0.816 to 0.754) from the national R value to the mean R value of the geographical grid boxes for cross-validation. However, an opposite trend appears for BPNN. On the other hand, the GRNN model obtains the highest standard deviation (Sd = 0.130) of R, meaning the biggest spatial variation of model performance. Meanwhile, the GWR model reports the smallest standard deviation (Sd = 0.079) of R, indicating that it is less sensitive to spatial location.

4.2. Mapping the mean distribution of $PM_{2.5}$ concentration

In Fig. 7, the yearly mean distributions of $PM_{2.5}$ concentration in China are mapped. The interpolated map presents a relatively coarse distribution of ground-level $PM_{2.5}$ concentrations, although it does not have much detailed spatial information, but is usually considered as a reference. The direct averaging of the satellite-derived $PM_{2.5}$ concentration does not share a similar spatial distribution with the interpolated map, with the most obvious difference being that Guangxi province has almost the same level of $PM_{2.5}$ as the BTH region. The reason for this is that the satellites can only detect the $PM_{2.5}$ pollution on certain days on which the AOD data are available. The results based on the proposed merging strategy share a similar spatial pattern with the interpolated map, but with many more details. Overall, the results suggest that the proposed pixel-based merging strategy is more effective for mapping the distribution of $PM_{2.5}$ concentration in China.

Based on the results obtained by the proposed merging strategy, a further analysis was undertaken. It can be seen that the spatial distribution of $PM_{2.5}$ concentration in 2014 is very similar to that in 2013. In most regions of China, the variation of $PM_{2.5}$ concentration falls in a range of -5 to $5 \mu g / m^3$ from 2013 to 2014, indicating that China was generally suffering from the same level of $PM_{2.5}$ pollution from 2013 to 2014. However, some spatial differences should be noted. There is a relatively large decrease ($10\sim 20 \mu g / m^3$) in the junction of Hebei, Shandong, and Henan provinces, but a contrasting trend can be seen in the junction of Hubei and Chongqing.

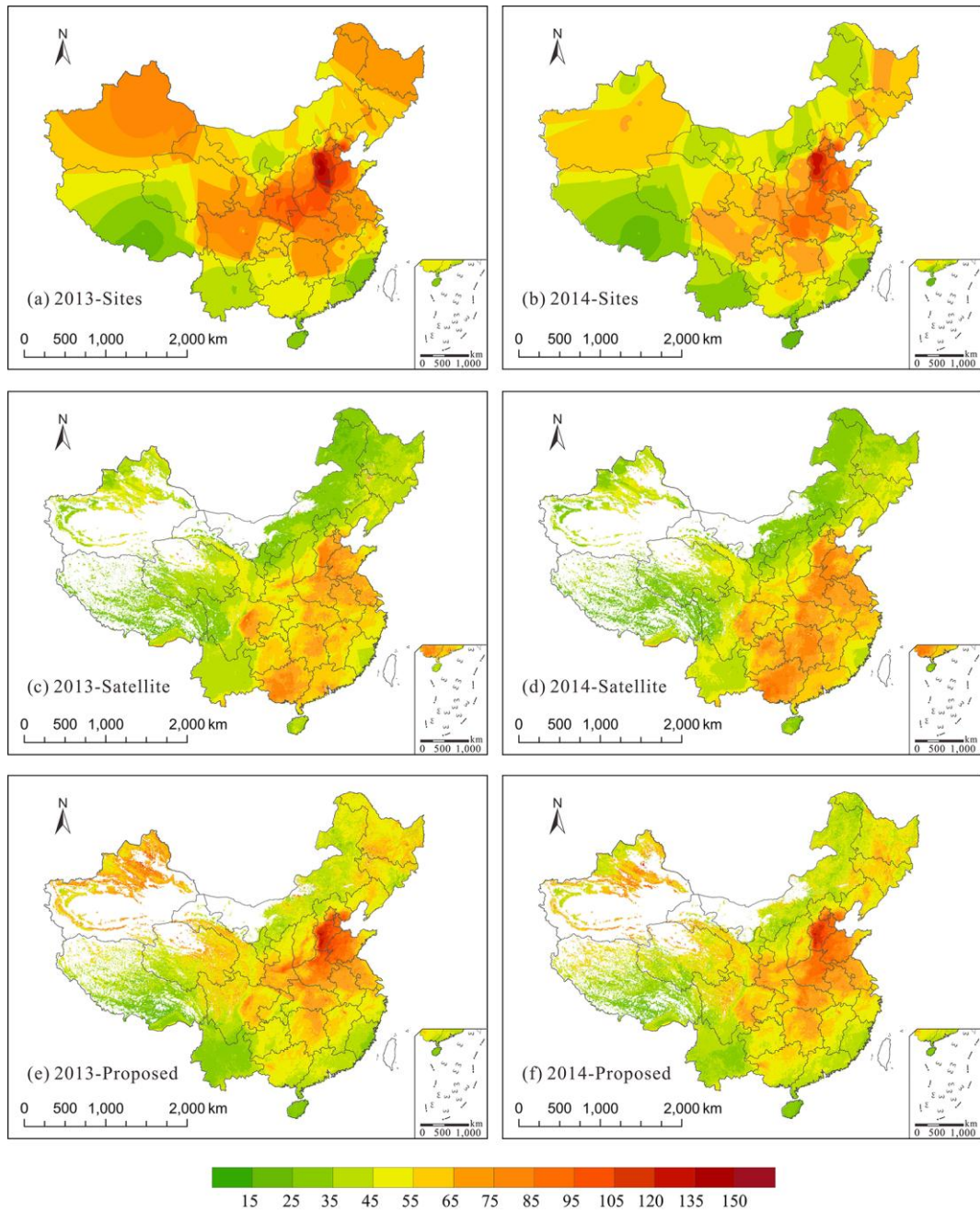


Fig. 7. Annual mean distribution of $PM_{2.5}$ concentration ($\mu g / m^3$) in China, (top) the results interpolated by ground site measurements, (middle) the direct averaging of satellite-derived $PM_{2.5}$ concentration, and (bottom) the mean distribution based on the proposed pixel-based merging strategy.

Spatially, the $PM_{2.5}$ pollution in West China is not as serious as that in Eastern China, which is accordance with the distribution of economic development and urbanization. Moreover, a strong north-to-south decreasing gradient is found, which agrees with the findings of previous studies (Lin et al., 2015). It should be noted that inner China generally suffers from a heavier

PM_{2.5} pollution level than the southeastern coast; for instance, Central China (Hunan, Hubei, and Henan provinces) has a higher level of PM_{2.5} concentration than Guangdong and Fujian provinces. In particular, a highly polluted region is located in the North China Plain, with a yearly average PM_{2.5} concentration of about 85~120 $\mu\text{g} / \text{m}^3$. Previous studies (Quan et al., 2011; Tao et al., 2012) showed that rapid industrialization and urbanization have led to serious PM_{2.5} pollution in this area. The cleanest regions are Hainan province, part of Yunnan province, and Tibet, with yearly mean PM_{2.5} concentrations of less than 35 $\mu\text{g} / \text{m}^3$.

The seasonal mean distribution of PM_{2.5} concentration in China was also mapped using the proposed pixel-based merging strategy. As presented in Fig. 8, 2013 and 2014 show similar seasonal trends. Winter is the most polluted season, whereas summer is the cleanest. According to previous studies (Han et al., 2010; Yu et al., 2011), this may be caused by winter heating in North China, Northeast China, and Northwest China.

The distribution of PM_{2.5} concentration is qualitatively similar to the station measurements. To make a further validation of the results, the R and RMSE values between the yearly and seasonal mean mapped PM_{2.5} and in situ PM_{2.5} were calculated, respectively. As Table 4 shows, the proposed merging strategy obtains better results than BCM at yearly and seasonal scale, with the R values all greater than 0.90, suggesting that the mapped PM_{2.5} distribution quantitatively agrees quite well with the station measurements. On the other side, the BCM method performs worst in winter, with the reason that many stations, on which the AOD data is missing during the whole winter, cannot be used for bias-correction. In fact, the BCM method has a systematic drawback being that many station measurements cannot be used for both model development and bias-correction due to the AOD absence during the whole study

period, whereas the proposed method can make the best use of the station measurements.

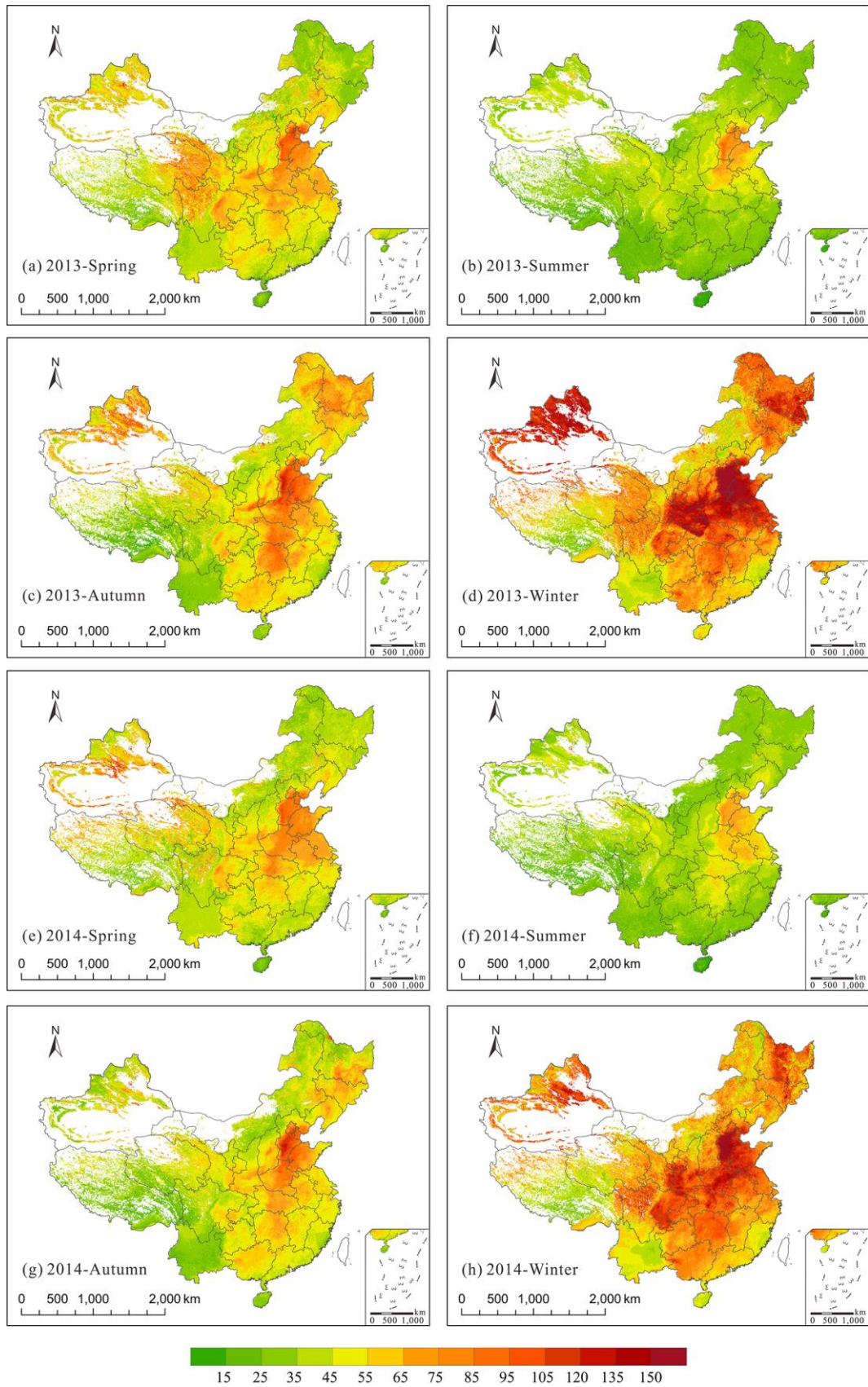


Fig. 8. Seasonal mean distribution of PM_{2.5} concentration ($\mu\text{g} / \text{m}^3$) in China.

Table 4. R and RMSE ($\mu\text{g} / \text{m}^3$) values between yearly and seasonal mean mapped PM_{2.5} and in situ PM_{2.5}.

method		2013					2014				
		All	Spring	Summer	Autumn	Winter	All	Spring	Summer	Autumn	Winter
Proposed	R	0.964	0.930	0.955	0.941	0.957	0.946	0.930	0.930	0.924	0.951
	RMSE	6.73	7.55	6.44	9.07	13.85	6.93	7.31	6.30	8.94	10.05
BCM	R	0.935	0.897	0.926	0.870	0.838	0.917	0.914	0.882	0.837	0.814
	RMSE	8.56	8.72	8.07	12.72	25.62	8.18	8.04	7.76	13.08	21.80

4.3. Discussion: comparison with previous studies

To date, there are two strategies that have been used for point-surface fusion for the estimation of ground-level PM_{2.5} concentration. One strategy is that the models are established based on all the data records collected from the whole study period (Gupta and Christopher, 2009a; Lin et al., 2015; Wu et al., 2012; Yao and Lu, 2014); the other strategy focuses on a daily basis (Ma et al., 2014; Ma et al., 2016; Song et al., 2014; Xie et al., 2015). Hence, our study can be classified as the former strategy. This strategy can predict the historical PM_{2.5} concentrations which cannot be provided by ground station measurements, whereas the latter strategy has an advantage in the real-time monitoring of PM_{2.5} pollution. To further validate our study, it was compared with one of the former studies (Lin et al., 2015) which focused on a national scale. To some degree, the model performance of the two strategies cannot be intercompared because of the huge differences, but we still made some attempts to qualitatively compare our results with those of the latter studies (Ma et al., 2014; Ma et al., 2016).

A good correlation (R=0.9) between annual mean observed and estimated PM_{2.5} in 2013 was reported in a previous study (Lin et al., 2015). Our results show a slight advantage in PM_{2.5} estimation, with R values between the GRNN-estimated PM_{2.5} and the corresponding observed PM_{2.5} of 0.929 during the same period. We also focused on the spatial pattern of

PM_{2.5} concentration in China. Our results are very similar to theirs, but are slightly lower along the Bo Hai Coast and higher in Shaanxi province. On the other hand, we also attempted to compare our results with those based on a daily basis and a grid technique (Ma et al., 2014; Ma et al., 2016). The R and RMSE values of these results are 0.80/0.89 and 32.98/27.42 $\mu\text{g}/\text{m}^3$, whereas we report 0.816 and 20.93 $\mu\text{g}/\text{m}^3$, respectively. There is a decrease in R value from their latter study to ours. However it should be noted that their study and ours have many significant differences in data and methods; for example, the AOD gap filling was undertaken in their study. Hence, the variation of R/RMSE cannot be the whole story. Compared with their former study, our results share a similar spatial distribution. However, a slightly higher level of PM_{2.5} concentration in the BTH region and a lower level in the Sichuan Basin are reported. Furthermore, our spatial pattern is also very like their results of the 10-year (2004–2013) PM_{2.5} mean distribution. The North China Plain has the highest level of PM_{2.5} concentration, and a gradual decrease appears from the north to the south.

5. Conclusions

To sum up, our study has several benefits and advantages. Firstly, we have introduced the new generalized regression neural network (GRNN) model to better describe the AOD-PM_{2.5} relationship. Secondly, the performance of various widely used models was evaluated and compared at national scale. Finally, a pixel-based merging strategy was proposed to effectively map the yearly and seasonal mean distribution of PM_{2.5} concentration in China.

With cross-validated R values of 0.488~0.552 and RMSEs of 30.80~31.51 $\mu\text{g}/\text{m}^3$, the conventional models did not report good results at national scale, although they did obtain some reasonable results under certain conditions in previous studies. In contrast the more

advanced models achieved better performances in $PM_{2.5}$ estimation, with R values of 0.610~0.816 and RMSEs of 20.93~28.68 $\mu g / m^3$. The proposed GRNN model obtained the best results, with the highest R (0.816) value and lowest RMSE (20.93 $\mu g / m^3$) among all the models. The R values between the yearly/seasonal mean mapped $PM_{2.5}$ and observed $PM_{2.5}$ were all greater than 0.90, indicating that the mapped $PM_{2.5}$ distribution agrees quite well with the station measurements. This study therefore has the capacity to provide reasonable information for the spatiotemporal analysis of $PM_{2.5}$ variation.

In future studies, we will focus on three aspects. Firstly, statistical methods will be introduced into filling the missing AOD data (Li et al., 2015; Shen et al., 2015; Zeng et al., 2013), because a wider coverage of satellite-based AOD could provide more comprehensive information for $PM_{2.5}$ estimation. Secondly, we will take more variables into consideration; for example, land use and population. More parameters associated with $PM_{2.5}$ pollution could lead to an improvement in $PM_{2.5}$ estimation accuracy. Finally, a long-term analysis of $PM_{2.5}$ pollution in China will be made to facilitate epidemiological studies about the impact of air pollution on public health, using the estimated $PM_{2.5}$ concentration at a 3-km resolution.

Acknowledgments

We would like to acknowledge the data providers of the Chinese National Environmental Monitoring Center (CNEMC), Goddard Space Flight Center Distributed Active Archive Center (GSFC DAAC) and US National Aeronautics and Space Administration (NASA) Data Center, respectively.

References

- Bartell, S.M., Longhurst, J., Tjoa, T., Sioutas, C., Delfino, R.J., 2013. Particulate air pollution, ambulatory heart rate variability, and cardiac arrhythmia in retirement community residents with coronary artery disease. *Environ. Health Perspect.* 121, 1135-1141.
- Beloconi, A., Kamarianakis, Y., Chrysoulakis, N., 2016. Estimating urban PM10 and PM2.5 concentrations, based on synergistic MERIS/AATSR aerosol observations, land cover and morphology data. *Remote Sens. Environ.* 172, 148-164.
- Benas, N., Beloconi, A., Chrysoulakis, N., 2013. Estimation of urban PM10 concentration, based on MODIS and MERIS/AATSR synergistic observations. *Atmos. Environ.* 79, 448-454.
- Chu, D.A., Kaufman, Y.J., Zibordi, G., Chern, J.D., Mao, J., Li, C., Holben, B.N., 2003. Global monitoring of air pollution over land from the Earth Observing System-Terra Moderate Resolution Imaging Spectroradiometer (MODIS). *J. Geophys. Res. Atmos.* 108.
- Cigizoglu, H.K., Alp, M., 2006. Generalized regression neural network in modelling river sediment yield. *Adv. Eng. Softw.* 37, 63-68.
- De Leeuw, J., Jia, H., Yang, L., Liu, X., Schmidt, K., Skidmore, A.K., 2006. Comparing accuracy assessments to infer superiority of image classification methods. *Int. J. Remote Sens.* 27, 223-232.
- Emili, E., Popp, C., Petitta, M., Riffler, M., Wunderle, S., Zebisch, M., 2010. PM10 remote sensing from geostationary SEVIRI and polar-orbiting MODIS sensors over the complex terrain of the European Alpine region. *Remote Sens. Environ.* 114, 2485-2499.
- Engel-Cox, J., Kim Oanh, N.T., van Donkelaar, A., Martin, R.V., Zell, E., 2013. Toward the next generation of air quality monitoring: Particulate Matter. *Atmos. Environ.* 80, 584-590.
- Gardner, M.W., Dorling, S.R., 1998. Artificial neural networks (the multilayer perceptron)—a review of applications in the atmospheric sciences. *Atmos. Environ.* 32, 2627-2636.
- Geng, G., Zhang, Q., Martin, R.V., van Donkelaar, A., Huo, H., Che, H., Lin, J., He, K., 2015. Estimating long-term PM2.5 concentrations in China using satellite-based aerosol optical depth and a chemical transport model. *Remote Sens. Environ.* 166, 262-270.
- Guo, J., Zhang, X., Che, H., Gong, S., An, X., Cao, C., Jie, G., Zhang, H., Wang, Y., Zhang, X., 2009. Correlation between PM concentrations and aerosol optical depth in eastern China. *Atmos. Environ.* 43, 5876-5886.
- Gupta, P., Christopher, S.A., 2009a. Particulate matter air quality assessment using integrated surface, satellite, and meteorological products: 2. A neural network approach. *J. Geophys. Res. Atmos.* 114, D20205.

Gupta, P., Christopher, S.A., 2009b. Particulate matter air quality assessment using integrated surface, satellite, and meteorological products: Multiple regression approach. *J. Geophys. Res. Atmos.* 114, D14205.

Gupta, P., Christopher, S.A., Wang, J., Gehrig, R., Lee, Y., Kumar, N., 2006. Satellite remote sensing of particulate matter and air quality assessment over global cities. *Atmos. Environ.* 40, 5880-5892.

Han, B., Kong, S., Bai, Z., Du, G., Bi, T., Li, X., Shi, G., Hu, Y., 2010. Characterization of Elemental Species in PM_{2.5} Samples Collected in Four Cities of Northeast China. *Water Air Soil Pollut.* 209, 15-28.

Hoff, R.M., Christopher, S.A., 2009. Remote Sensing of Particulate Pollution from Space: Have We Reached the Promised Land? *J. Air Waste Manage. Assoc.* 59, 645-675.

Hu, X., Waller, L.A., Al-Hamdan, M.Z., Crosson, W.L., Estes Jr, M.G., Estes, S.M., Quattrochi, D.A., Sarnat, J.A., Liu, Y., 2013. Estimating ground-level PM_{2.5} concentrations in the southeastern U.S. using geographically weighted regression. *Environ. Res.* 121, 1-10.

Hu, X., Waller, L.A., Lyapustin, A., Wang, Y., Al-Hamdan, M.Z., Crosson, W.L., Estes Jr, M.G., Estes, S.M., Quattrochi, D.A., Puttaswamy, S.J., Liu, Y., 2014a. Estimating ground-level PM_{2.5} concentrations in the Southeastern United States using MAIAC AOD retrievals and a two-stage model. *Remote Sens. Environ.* 140, 220-232.

Hu, X., Waller, L.A., Lyapustin, A., Wang, Y., Liu, Y., 2014b. 10-year spatial and temporal trends of PM_{2.5} concentrations in the southeastern US estimated using high-resolution satellite data. *Atmos. Chem. Phys.* 14, 6301-6314.

Kisi, O., Kerem Cigizoglu, H., 2007. Comparison of different ANN techniques in river flow prediction. *Civ. Eng. Environ. Syst.* 24, 211-231.

Kloog, I., Chudnovsky, A.A., Just, A.C., Nordio, F., Koutrakis, P., Coull, B.A., Lyapustin, A., Wang, Y., Schwartz, J., 2014. A new hybrid spatio-temporal model for estimating daily multi-year PM_{2.5} concentrations across northeastern USA using high resolution aerosol optical depth data. *Atmos. Environ.* 95, 581-590.

Kloog, I., Koutrakis, P., Coull, B.A., Lee, H.J., Schwartz, J., 2011. Assessing temporally and spatially resolved PM_{2.5} exposures for epidemiological studies using satellite aerosol optical depth measurements. *Atmos. Environ.* 45, 6267-6275.

Levy, R.C., Mattoo, S., Munchak, L.A., Remer, L.A., Sayer, A.M., Patadia, F., Hsu, N.C., 2013. The Collection 6 MODIS aerosol products over land and ocean. *Atmos. Meas. Tech.* 6, 2989-3034.

Li, C., Hsu, N.C., Tsay, S.-C., 2011. A study on the potential applications of satellite data in air

quality monitoring and forecasting. *Atmos. Environ.* 45, 3663-3675.

Li, C., Mao, J., Lau, A.K.H., Yuan, Z., Wang, M., Liu, X., 2005. Application of MODIS satellite products to the air pollution research in Beijing. *Sci. China Earth Sci.* 48, 209-219.

Li, X., Shen, H., Zhang, L., Li, H., 2015. Sparse-based reconstruction of missing information in remote sensing images from spectral/temporal complementary information. *ISPRS J. Photogramm.* 106, 1-15.

Li, Z., Zhang, Y., Shao, J., Li, B., Hong, J., Liu, D., Li, D., Wei, P., Li, W., Li, L., Zhang, F., Guo, J., Deng, Q., Wang, B., Cui, C., Zhang, W., Wang, Z., Lv, Y., Xu, H., Chen, X., Li, L., Qie, L., 2016. Remote sensing of atmospheric particulate mass of dry PM_{2.5} near the ground: Method validation using ground-based measurements. *Remote Sens. Environ.* 173, 59-68.

Lin, C., Li, Y., Yuan, Z., Lau, A.K.H., Li, C., Fung, J.C.H., 2015. Using satellite remote sensing data to estimate the high-resolution distribution of ground-level PM_{2.5}. *Remote Sens. Environ.* 156, 117-128.

Liu, Y., Franklin, M., Kahn, R., Koutrakis, P., 2007. Using aerosol optical thickness to predict ground-level PM_{2.5} concentrations in the St. Louis area: A comparison between MISR and MODIS. *Remote Sens. Environ.* 107, 33-44.

Liu, Y., Park, R.J., Jacob, D.J., Li, Q., Kilaru, V., Sarnat, J.A., 2004. Mapping annual mean ground-level PM_{2.5} concentrations using Multiangle Imaging Spectroradiometer aerosol optical thickness over the contiguous United States. *J. Geophys. Res. Atmos.* 109, D22206.

Liu, Y., Sarnat, J.A., Kilaru, V., Jacob, D.J., Koutrakis, P., 2005. Estimating Ground-Level PM_{2.5} in the Eastern United States Using Satellite Remote Sensing. *Environ. Sci. Technol.* 39, 3269-3278.

Liu, Y., Schichtel, B.A., Koutrakis, P., 2009. Estimating Particle Sulfate Concentrations Using MISR Retrieved Aerosol Properties. *IEEE J. Sel. Topics Appl. Earth Observ. in Remote Sens.* 2, 176-184.

Livingston, J.M., Redemann, J., Shinozuka, Y., Johnson, R., Russell, P.B., Zhang, Q., Mattoo, S., Remer, L., Levy, R., Munchak, L., Ramachandran, S., 2014. Comparison of MODIS 3 km and 10 km resolution aerosol optical depth retrievals over land with airborne sunphotometer measurements during ARCTAS summer 2008. *Atmos. Chem. Phys.* 14, 2015-2038.

Ma, Z., Hu, X., Huang, L., Bi, J., Liu, Y., 2014. Estimating Ground-Level PM_{2.5} in China Using Satellite Remote Sensing. *Environ. Sci. Technol.* 48, 7436-7444.

Ma, Z., Hu, X., Sayer, A.M., Levy, R., Zhang, Q., Xue, Y., Tong, S., Bi, J., Huang, L., Liu, Y., 2016. Satellite-Based Spatiotemporal Trends in PM_{2.5} Concentrations: China, 2004-2013.

Environ. Health Perspect. 124, 184-192.

Martin, R.V., 2008. Satellite remote sensing of surface air quality. *Atmos. Environ.* 42, 7823-7843.

Molod, A., Takacs, L., Suarez, M., Bacmeister, J., 2015. Development of the GEOS-5 atmospheric general circulation model: evolution from MERRA to MERRA2. *Geosci. Model Dev.* 8, 1339-1356.

Ordieres, J.B., Vergara, E.P., Capuz, R.S., Salazar, R.E., 2005. Neural network prediction model for fine particulate matter (PM_{2.5}) on the US–Mexico border in El Paso (Texas) and Ciudad Juárez (Chihuahua). *Environ. Modell. Softw.* 20, 547-559.

Peng, J., Chen, S., Lü, H., Liu, Y., Wu, J., 2016. Spatiotemporal patterns of remotely sensed PM_{2.5} concentration in China from 1999 to 2011. *Remote Sens. Environ.* 174, 109-121.

Quan, J., Zhang, Q., He, H., Liu, J., Huang, M., Jin, H., 2011. Analysis of the formation of fog and haze in North China Plain (NCP). *Atmos. Chem. Phys.* 11, 8205-8214.

Reich, S.L., Gomez, D.R., Dawidowski, L.E., 1999. Artificial neural network for the identification of unknown air pollution sources. *Atmos. Environ.* 33, 3045-3052.

Remer, L.A., Kaufman, Y.J., Tanré D., Mattoo, S., Chu, D.A., Martins, J.V., Li, R.R., Ichoku, C., Levy, R.C., Kleidman, R.G., Eck, T.F., Vermote, E., Holben, B.N., 2005. The MODIS Aerosol Algorithm, Products, and Validation. *J. Atmos. Sci.* 62, 947-973.

Rienecker, M.M., Suarez, M.J., Gelaro, R., Todling, R., Bacmeister, J., Liu, E., Bosilovich, M.G., Schubert, S.D., Takacs, L., Kim, G-K., Bloom, S., Chen, J., Collins, D., Conaty, A., da Silva, A., Gu, W., Joiner, J., Koster, R.D., Lucchesi, R., Molod, A., Owens, T., Pawson, S., Pegion, P., Redder, C.R., Reichle, R., Robertson, F.R., Ruddick, A.G., Sienkiewicz, M., Woollen, J., 2011. MERRA: NASA's Modern-Era Retrospective Analysis for Research and Applications. *J. Climate* 24, 3624-3648.

Rodriguez, J.D., Perez, A., Lozano, J.A., 2010. Sensitivity Analysis of k-Fold Cross Validation in Prediction Error Estimation. *IEEE Trans. Pattern Anal. Mach. Intell.* 32, 569-575.

Sacks, J.D., Stanek, L.W., Luben, T.J., Johns, D.O., Buckley, B.J., Brown, J.S., Ross, M., 2011. Particulate matter-induced health effects: who is susceptible? *Environ. Health Perspect.* 119, 446-454.

Shen, H., Li, X., Cheng, Q., Zeng, C., Yang, G., Li, H., Zhang, L., 2015. Missing Information Reconstruction of Remote Sensing Data: A Technical Review. *IEEE Geosci. Remote Sens. Mag.* 3, 61-85.

Shen, H., Wu, P., Liu, Y., Ai, T., Wang, Y., Liu, X., 2013. A spatial and temporal reflectance fusion

- model considering sensor observation differences. *Int. J. Remote Sens.* 34, 4367-4383.
- Song, W., Jia, H., Huang, J., Zhang, Y., 2014. A satellite-based geographically weighted regression model for regional PM_{2.5} estimation over the Pearl River Delta region in China. *Remote Sens. Environ.* 154, 1-7.
- Specht, D.F., 1991. A general regression neural network. *IEEE Trans. Neural. Netw.* 2, 568-576.
- Specht, D.F., 1993. The general regression neural network—Rediscovered. *Neural Networks* 6, 1033-1034.
- Tao, M., Chen, L., Su, L., Tao, J., 2012. Satellite observation of regional haze pollution over the North China Plain. *J. Geophys. Res. Atmos.* 117.
- Tian, J., Chen, D., 2010. A semi-empirical model for predicting hourly ground-level fine particulate matter (PM_{2.5}) concentration in southern Ontario from satellite remote sensing and ground-based meteorological measurements. *Remote Sens. Environ.* 114, 221-229.
- van Donkelaar, A., Martin, R.V., Brauer, M., Kahn, R., Levy, R., Verduzco, C., Villeneuve, P.J., 2010. Global estimates of ambient fine particulate matter concentrations from satellite-based aerosol optical depth: development and application. *Environ. Health Perspect.* 118, 847-855.
- van Donkelaar, A., Martin, R.V., Pasch, A.N., Szykman, J.J., Zhang, L., Wang, Y.X., Chen, D., 2012. Improving the Accuracy of Daily Satellite-Derived Ground-Level Fine Aerosol Concentration Estimates for North America. *Environ. Sci. Technol.* 46, 11971-11978.
- Wang, J., Christopher, S.A., 2003. Intercomparison between satellite-derived aerosol optical thickness and PM_{2.5} mass: Implications for air quality studies. *Geophys. Res. Lett.* 30.
- Wang, Z., Chen, L., Tao, J., Zhang, Y., Su, L., 2010. Satellite-based estimation of regional particulate matter (PM) in Beijing using vertical-and-RH correcting method. *Remote Sens. Environ.* 114, 50-63.
- Wen, J., Zhao Jia, L., Luo Si, W., Han, Z., 2000. The improvements of BP neural network learning algorithm, 5th International Conference on Signal Processing Proceedings, 2000. WCCC-ICSP 2000. , pp. 1647-1649 vol.1643.
- Wu, P., Shen, H., Ai, T., Liu, Y., 2013. Land-surface temperature retrieval at high spatial and temporal resolutions based on multi-sensor fusion. *Int. J Digit. Earth* 6, 113-133.
- Wu, P., Shen, H., Zhang, L., Göttsche, F.-M., 2015. Integrated fusion of multi-scale polar-orbiting and geostationary satellite observations for the mapping of high spatial and temporal resolution land surface temperature. *Remote Sens. Environ.* 156, 169-181.

- Wu, Y., Guo, J., Zhang, X., Tian, X., Zhang, J., Wang, Y., Duan, J., Li, X., 2012. Synergy of satellite and ground based observations in estimation of particulate matter in eastern China. *Sci. Total Environ.* 433, 20-30.
- Xie, Y., Wang, Y., Zhang, K., Dong, W., Lv, B., Bai, Y., 2015. Daily estimation of ground-level PM_{2.5} concentrations over Beijing using 3 km resolution MODIS AOD. *Environ. Sci. Technol.* 49, 12280-12288.
- Yao, L., Lu, N., 2014. Spatiotemporal distribution and short-term trends of particulate matter concentration over China, 2006–2010. *Environ. Sci. Pollut. Res.* 21, 9665-9675.
- You, W., Zang, Z., Pan, X., Zhang, L., Chen, D., 2015a. Estimating PM_{2.5} in Xi'an, China using aerosol optical depth: A comparison between the MODIS and MISR retrieval models. *Sci. Total Environ.* 505, 1156-1165.
- You, W., Zang, Z., Zhang, L., Li, Z., Chen, D., Zhang, G., 2015b. Estimating ground-level PM₁₀ concentration in northwestern China using geographically weighted regression based on satellite AOD combined with CALIPSO and MODIS fire count. *Remote Sens. Environ.* 168, 276-285.
- Yu, X., 1992. Can backpropagation error surface not have local minima. *IEEE Trans. Neural. Netw.* 3, 1019-1021.
- Yu, Y., Schleicher, N., Norra, S., Fricker, M., Dietze, V., Kaminski, U., Cen, K., Stuben, D., 2011. Dynamics and origin of PM_{2.5} during a three-year sampling period in Beijing, China. *J. Environ. Monit.* 13, 334-346.
- Yuan, Y., Liu, S., Castro, R., Pan, X., 2012. PM_{2.5} Monitoring and Mitigation in the Cities of China. *Environ. Sci. Technol.* 46, 3627-3628.
- Zeng, C., Shen, H., Zhang, L., 2013. Recovering missing pixels for Landsat ETM + SLC-off imagery using multi-temporal regression analysis and a regularization method. *Remote Sens. Environ.* 131, 182-194.
- Zhang, Y., Cao, F., 2015. Fine particulate matter (PM_{2.5}) in China at a city level. *Sci. Rep.* 5, 14884.
- Zhang, Y., Li, Z., 2015. Remote sensing of atmospheric fine particulate matter (PM_{2.5}) mass concentration near the ground from satellite observation. *Remote Sens. Environ.* 160, 252-262.
- Zheng, Y., Zhang, Q., Liu, Y., Geng, G., He, K., 2016. Estimating ground-level PM_{2.5} concentrations over three megalopolises in China using satellite-derived aerosol optical depth measurements. *Atmos. Environ.* 124, Part B, 232-242.